Communication

Nanometric Layers for Direct, Signal-On, Selective, and Sensitive Electrochemical Detection of Oligonucleotides Hybridization

Gre#gory March, Vincent Noe#l, Benoi#t Piro, Steeve Reisberg, and Minh-Chau Pham

J. Am. Chem. Soc., **2008**, 130 (47), 15752-15753 • DOI: 10.1021/ja8047255 • Publication Date (Web): 31 October 2008

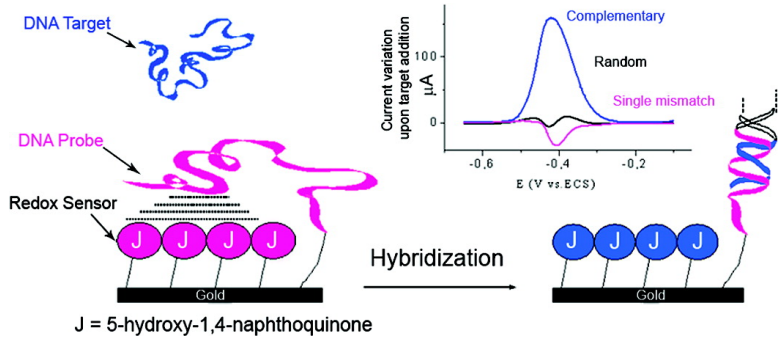

More About This Article

Additional resources and features associated with this article are available within the HTML version:

- Supporting Information
- Access to high resolution figures
- Links to articles and content related to this article
- Copyright permission to reproduce figures and/or text from this article

View the Full Text HTML

J|A|C|S
COMMUNICATIONS

Published on Web 10/31/2008

Nanometric Layers for Direct, Signal-On, Selective, and Sensitive Electrochemical Detection of Oligonucleotides Hybridization

Grégory March, Vincent Noël, Benoît Piro, Steeve Reisberg, and Minh-Chau Pham*

Interfaces, Traitement, Organisation et Dynamiques des Systèmes, Université Paris 7 - Denis Diderot, UMR 7086, 15 rue Jean de Baif, 75205 Paris cedex 13, France

Received June 20, 2008; E-mail: mcpham@univ-paris-diderot.fr

In the present paper we report an original reagentless electrochemical DNA biosensor, based on an electroactive self-assembled 5-hydroxy-3-hexanedithiol-1,4-naphthoquinone (JUG_{thio}) monolayer, which achieves highly sensitive and selective signal-on detection and may also be easily transposable for protein recognition. In the field of label-free electrochemical DNA biosensors, signal-on devices are preferable to signal-off ones in that false positives are less likely.[1,2] The main aim is to find sensitive interfaces with charge transfer properties which change depending on the nature and the quantity of the DNA target.[3−5] In the last few years, a new direction towards signal-on sensors is to exploit the differences in the physical properties of single-stranded DNA compared to double-stranded DNA.[6−9] One of the first sensors using this new approach was based upon a DNA-PEG-DNA "wrap" format.[8] In this sensor, the immobilized DNA is composed of two hybridization sequences ("capture" and "probe") connected by a linker (PEG) and a redox probe reporter attached to the end of the probe strand. The redox probe reporter is brought close to an electrode upon hybridization, producing a signal-on sensor for a target concentration up to few nanomoles. Another elegant way to realize label-free electrochemical DNA sensors might be to use dense monolayers in which a redox center is in the outside part of the self-assembled monolayer (SAM) (cf. scheme 1).

To the best of our knowledge there is no published system using the electroactivity of the substrate monolayer itself as a signal-on transducer of DNA hybridization. As part of the general strategy of our group aimed at developing label-free electrochemical biosensors, we undertook to investigate whether a JUG_{thio} monolayer self-assembled with a DNA probe on gold could produce a biosensitive interface.

The biosensor consists of a mixed monolayer of JUG_{thio} and single-stranded oligonucleotides modified in the 3′ position by an alkylthiol (HS-ss-ODN) (Scheme 1). Oligonucleotide sequences are detailed below (bases really used, in bold; others are spacers to avoid edge effects; mismatches, underlined). The probe sequence is HS-ss-GEM (5′- TC**G CAC CCA TCT CTC TCC TTC T**AG CCT -3′C_9H_{18}SH), the complementary target HIV (3′- **CG TGG GTA GAG AGA GGA AGA** -5′), the mismatch sequence MHIV (3′- **CG TGG GTA AAG AGA GGA AGA** -5′). and the random sequence RAND (3′- **CG TAA ATG ATC CTT CAA CTA** -5′).

JUG_{thio} SAMs were obtained by immersing a 1 cm^2 freshly washed and pretreated gold electrode (see Supporting Information, SI) in a 1 mg/mL JUG_{thio} solution in ethylacetate overnight with stirring and an Ar atmosphere. Square-wave voltammetry (SWV) was performed on JUG_{thio} SAMs in phosphate buffer medium (PBS, pH 7.4) from 0.00 V to −0.65 V (vs SCE). One reduction peak appears at ∼ −0.44 V, corresponding to the redox process of the quinone group. In the following, it is the change in intensity of this peak that will be considered as significant for grafting and hybridization experiments. Then, HS-ss-ODN probe strands were self-assembled onto the JUG_{thio}-modified gold electrode. We assume that the mixed monolayer is obtained by the partial replacement of JUG_{thio} by HS-ss-ODN. The total charge of the monolayer obtained by cyclic voltammetric experiments is not significantly different after the exchange reaction, indicating that very few ODN probes are immobilized. However, SWV experiments show that the current diminishes after the self-assembly of HS-ss-ODN (see SI).

Scheme 1. Electrochemical Detection Strategy Based on the Change in Electroactivity of Self-Assembled JUG_{thio} Monolayers upon Hybridization

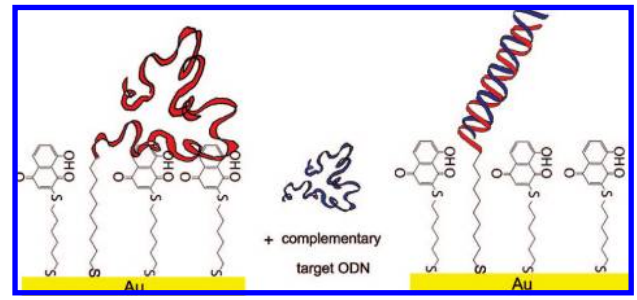

Target probes 0.1 μM of HIV (full complementary), RAND (random), or MHIV (single mismatch) are then added (see SI). In the case of MHIV, hybridization was performed at 50°C, instead of room temperature, and the mixture was slowly cooled to 37°C to improve the selectivity. SWV was applied after the hybridization. We calculated the differential peak current ($\Delta I = I_{HYB} - I_{GEM}$), with I_{HYB} and I_{GEM} as the peak currents after and before, respectively, target addition. As shown in Figure 1, the HIV target leads to a drastic increase in intensity of the peak at −0.44 V (*i.e.*, signal-on detection), whereas the RAND sequence does not lead to a significant current change. In the case of MHIV, a signal decrease is noted. This decrease is as great as that observed in a blank experiment when JUG_{thio} SAMs are treated at 50°C in PBS without MHIV (thermal SAM desorption). This system exhibits signal-on detection, that is to say, an enhancement of peak current after hybridization with the full complementary target and no change after addition of a random target. Moreover, this system is very selective in that it allows discrimination between target probes which differ by only one base.

These results were supported by quantitative measurements, performed by fluorescence spectroscopy (see SI). Fluorescent targets are modified with a BODIPY 650/675 molecule on their 5′-end. After the hybridization, three washing steps (PBS at 25°C) were performed followed by a denaturation step (80°C in pure water). At each step, the solution is analyzed by fluorescence measurements. Denaturation of all the hybridized fluorescent ODN leads to the dehybridization of ∼10 pmol cm^{-2} for complementary strands and to a negligible amount for the random sequence and the mismatch sequence. These results demonstrate that hybridization is truly

10.1021/ja8047255 CCC: $40.75

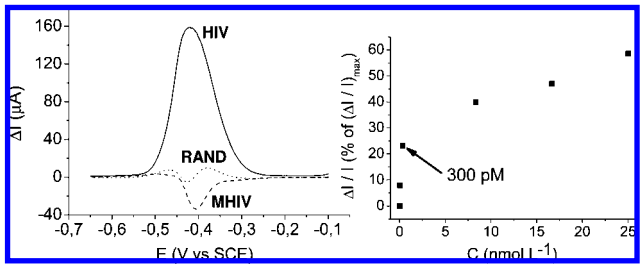

Figure 1. (Left) Differential peak current ($\Delta I = I_{HYB} - I_{GEM}$), with I_{HYB} and I_{GEM} as the peak currents after and before hybridization, respectively, after addition of HIV, RAND, and MHIV. (Right) Differential current $\Delta I/I$ (expressed as a percentage of the maximum at 100 nM), measured for different HIV concentrations.

responsible for the current increase in the case of the full complementary strand, whereas the addition of the random sequence, which does not hybridize, leads to negligible current change.

To determine the detection threshold of the system, the SWV current response was measured as a function of the full complementary target strand concentration. Results are shown in Figure 1 for concentrations between 30 pM and 25 nM and are expressed as a percentage of the maximum of $\Delta I/I_{GEM}$. The current response remains low, below 300 pM, and then follows a sharp increase until a maximum is reached at ~100 nM (see SI). We estimate the detection threshold to be ~300 pM.

All the already published reagentless monolayer systems showing signal-on transduction are based on redox molecules grafted onto the DNA probe. The aim is to create an ad-hoc ODN structure which allows the redox probe to reach the vicinity of the electrode surface after hybridization. This strategy exploits the special structural properties of DNA strands, which become rigid upon double helix formation. Our approach is totally different, because the transduction principle is based on the modification of the intrinsic properties of JUG_{thio} which stays at the same distance from the electrode.

In previous work,[10] we analyzed the electron transfer kinetics of a pure JUG_{thio} monolayer self-assembled on gold. A kinetic analysis of the redox reactions involving both electron and proton transfers revealed unusual behaviour of this molecule, due to the presence of several inter- and intramolecular hydrogen bonds, especially in neutral buffered solutions. These results show that the JUG_{thio} redox kinetics is controlled by a chemical rate-determining step resulting from the necessity to disrupt these bonds in the monolayer before charge transfer.

Single-stranded ODN (ssODN) is considered to behave as a classical polymer chain. This means that, in the vermicular model, ssODN could be characterized by its contour length (L) and its persistence length (p). L varies slightly between dsODN and ssODN, but p varies dramatically between the single and the double strand (dsODN) conformation. Indeed, p_{dsODN} is 50 nm, whereas p_{ssODN} varies between 0.8 and 8 nm, depending on the ionic strength.[11−13] Here, the salt concentration is ~0.13 M, and 20 nucleobases are involved in hybridization. In this case, one finds 8.6 and 6.8 nm for L_{ssODN} and L_{dsODN}, respectively (see SI). Therefore, L_{ssODN} is much greater than p_{ssODN} (1 nm in our case), and the chain behaves as a coil. Conversely, for a dsODN, L_{dsODN} is much less than 50 nm (p_{dsODN}). The double strand is straight and rigid. Hence, the single strand has a high degree of freedom (increased by the length and the flexibility of the alkylthiol linker) and is able to interact with molecules on the surface. Conversely, the double strand is rigid, and most of the probe hydrogen bonding sites are involved in Watson−Crick base pairing with the target.

The ability to modulate the electroactivity of JUG_{thio} by hydrogen bonding and the specific capacity of the grafted ODN probe to interact with the monolayer surface suggest an interpretation of the signal-on behavior towards hybridization. Indeed, before hybridization, the single strand can interact with JUG_{thio} and slow down the redox reaction. This phenomenon can explain the decrease in the observed SQW peak current upon probe grafting. When the complementary target is added, the formation of the double helix eliminates the single strand/JUG_{thio} interactions and the JUG_{thio} redox rate increases.

However, the above discussion does not take into account the negative charge on the phosphodiester ODN backbone. The high ionic strength, used in this study, is presumed to screen electrostatic effects at sub-nanometric distances. Therefore, experiments with peptide nucleic acid are currently being performed in the laboratory to check this point. Another important concept to be understood is the exact molecular nature of the interaction between the single strand and JUG_{thio}.

In the field of label-free electrochemical DNA sensors based on monolayers, the JUG_{thio} system is the only architecture allowing signal-on detection without requiring probe modification. Moreover, when taken with the observation that any single-stranded DNA or RNA sequence, including aptamer sequences, can interact with the JUG_{thio} monolayer, and given that the target-binding-induced folding of an aptamer should also disrupt interfacial hydrogen bonding, this direct transduction principle may also prove appropriate for the detection of proteins, small nonelectroactive molecules, and other non-nucleic acid targets, even in complex clinical samples.

Supporting Information Available: Experimental details. This material is available free of charge via the Internet at http://pubs.acs.org.

References

(1) Sassolas, A.; Leca-Bouvier, B. D.; Blum, L. J. *Chem. Rev.* **2008**, *108*, 109–139.
(2) Wang, J. *Chem.—Eur. J.* **1999**, *5*, 1681–1685.
(3) Piro, B.; Reisberg, S.; Noel, V.; Pham, M. C. *Biosens. Bioelectron.* **2007**, *22*, 3126–3631.
(4) Thompson, L. A.; Kowalik, J.; Josowicz, M.; Janata, J. *J. Am. Chem. Soc.* **2003**, *125*, 324–325.
(5) Korri-Youssoufi, H.; Garnier, P.; Srivastava, P.; Godillot, P.; Yassar, A. *J. Am. Chem. Soc.* **1997**, *119*, 7388–7389.
(6) Gooding, J. J.; Garry, C. K. *J. Mater Chem.* **2005**, *15*, 4876–4880.
(7) Fan, C.; Plaxco, K. W.; Heeger, A. J. *Proc. Natl. Acad. Sci. U.S.A.* **2003**, *100*, 9134–9137.
(8) Immoos, C. E.; Lee, S. J.; Grinstaff, M. W. *J. Am. Chem. Soc.* **2004**, *126*, 10814–10815.
(9) Xiao, Y.; Qu, X.; Plaxco, K. W.; Heeger, A. J. *J. Am. Chem. Soc.* **2007**, *129*, 11896–11897.
(10) March, G.; Reisberg, S.; Piro, B.; Pham, M.-C.; Delamar, M.; Noel, V.; Odenthal, K.; Hibbert, D. B.; Gooding, J. J. *J. Electroanal. Chem* **2008**, *622*, 37–43.
(11) Tinland, B.; Pluen, A.; Sturm, J.; Weill, G. *Macromolecules* **1997**, *30*, 5763–5765.
(12) Smith, S. B.; Cui, Y.; Bustamante, C. *Science* **1996**, *271*, 795–799.
(13) Bednar, J.; Furrer, P.; Katritch, V.; Stasiak, A. Z.; Dubochet, J.; Stasiak, A. *J. Mol. Biol.* **1995**, *254*, 579–594.

JA8047255